Available online at www.sciencedirect.com
ScienceDirect
Scripta Materialia 63 (2010) 101–104
Scripta MATERIALIA
www.elsevier.com/locate/scriptamat

Scaling of the ductility with yield strength in nanostructured Cu/Cr multilayer films

J.Y. Zhang, X. Zhang, G. Liu,* G.J. Zhang and J. Sun**

State Key Laboratory for Mechanical Behavior of Materials, Xi'an Jiaotong University, Xi'an 710049, People's Republic of China

Received 27 February 2010; accepted 6 March 2010
Available online 11 March 2010

At a constant modulation period (λ), nanostructured Cu/Cr multilayer films exhibit ductility scaling linearly with yield strength that varies with modulation ratio. The films with different λ have their own scaling relationship. The scaling slope for $\lambda = 25$ nm is much sharper than that for $\lambda = 50$ nm, indicating that a stronger interface constraint causes a larger reduction in ductility. These scaling relationships can be understood by referring to macroscopic fracture models based on a critical stress criterion.

Keywords: Nanostructured multilayers; Ductility; Strength; Modulation ratio; Scaling relationship

Nanostructured multilayer films (NMFs) are used in a variety of applications because of the improved capability of tailoring the fabrication of these structures to meet specific property needs [1–4]. For NMFs with a constant modulation ratio of $\eta = 1$, the decrease in the modulation period (λ) was found to increase the strength/hardness because the nucleation and motion of dislocations within the films are strongly suppressed by increased layer-to-layer interfaces [5–10]. However, there have been few reports to quantitatively show the dependence of ductility on the modulation period and modulation ratio in the NMFs. It is also not clear how the ductility of NMFs is related to the strength, which limits the artificial controlling of the constituent layers to achieve an optimized combination of ductility and strength in the NMFs.

In this paper, we report on the variation of yield strength and ductility with modulation ratio in polyimide-supported Cu/Cr NMFs with $\lambda = 25$ and 50 nm, respectively. A wide range of both ductility and yield strength has been developed by artificially tailoring η (defined as the ratio of Cr layer thickness to Cu layer thickness, $\eta = h_{Cr}/h_{Cu}$) from 0.11 to 3. The ductility was found to scale with the yield strength for a constant λ and the NMFs with a thinner λ exhibited a sharper scaling slope. The η-dependent strength was assessed based on a dislocation strengthening model and the variation of ductility with modulation ratio has been quantitatively related to the evolution of fracture mode at microstructural level.

Polyimide-supported Cu/Cr NMFs with constant λ ($\lambda = 25$ and 50 nm) but different η of 0.11, 0.2, 0.33, 0.5, 1.0, 2.0 and 3.0 were, respectively, synthesized by means of direct current (DC) magnetron sputtering at room temperature. The Cr layer was first deposited on the substrate and finally the topmost layer of the multilayer was Cu. The total thickness of the Cu/Cr NMFs was kept to about 500 nm. The as-deposited multilayer films were annealed at 150 °C for 2 h in a high vacuum environment (less than 10^{-8} mbar) to stabilize the microstructure. X-ray diffraction (XRD) revealed a strong <1 1 1> out-of-plane texture for the Cu layers and a weak <1 1 0> out-of-plane texture for Cr layers, while the in-plane orientations are random. By using XRD and the "$\sin^2\psi$ method", the residual tensile stresses were determined to be about 200 ± 100 MPa for all the annealed Cu/Cr NMFs with different λ and η, which is far lower than their yield strength. Some typical cross-section transmission electron microscopy (TEM) micrographs of the NMFs are presented in Figure 1, in which one can see the clear alternate layers. The average grain sizes of both Cu and Cr scale with layer thickness. Some bright fringes are observed along the interface between the Cu layer and Cr layer (e.g. in Fig. 1(a)). These very thin disordered regions (with thickness of ~2 nm) are formed from intermixing between Cu and Cu driven by the surface energy during the nonequilibrium deposition process [11]. Similar phe-

* Corresponding author.
** Corresponding author. E-mail: lgsammer@mail.xjtu.edu.cn; junsun@mail.xjtu.edu.cn

1359-6462/$ - see front matter © 2010 Acta Materialia Inc. Published by Elsevier Ltd. All rights reserved.
doi:10.1016/j.scriptamat.2010.03.024

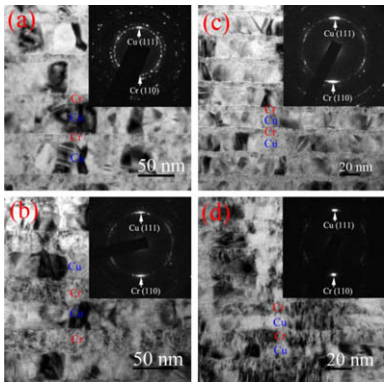

Figure 1. Bright-field cross-sectional TEM micrographs showing the typical microstructure of Cu/Cr NMFs with different λs ((a) and (b): $\lambda = 50$ nm; (c) and (d): $\lambda = 25$ nm) and different ηs ((a) and (c): $\eta = 0.33$; (b) and (d): $\eta = 1.0$). The inset shows the corresponding selected area diffraction patterns.

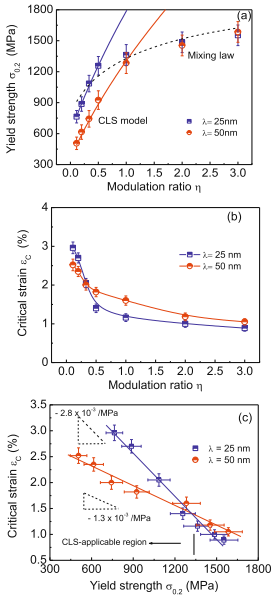

Figure 2. Dependence of (a) $\sigma_{0.2}$ and (b) ε_C on η for the Cu/Cr NMFs with $\lambda = 25$ and 50 nm, respectively. In (a), solid curves are calculations from CLS model and dash curve is from the simple mixing law. (c) Scaling relationship between ε_C and $\sigma_{0.2}$ in the Cu/Cr NMFs with $\lambda = 25$ and 50 nm.

nomena have been observed in other binary immiscible metallic systems, such as Ag/Ni [11] and Cu/Fe [12]. Further analyses showed that there are no obvious differences in chemical composition and in thickness between the intermixed layers before and after annealing treatment. This indicates that the present annealing treatment, performed at relative low temperature (150 °C), did not demix the intermixed layers.

Uniaxial tensile testing was carried out by using a Micro-Force Test System (MTS® Tytron 250) at a constant strain rate of 1×10^{-4} s^{-1}. Dogbone-shaped samples for testing had a total length of 65 mm, and a gauge section of 30 mm in length and 4 mm in width. During tensile testing, the force and displacement were automatically recorded by machine and a high-resolution laser detecting system, respectively. The measurements can be subsequently converted into stress–strain curves of the films by subtracting the load–displacement data of the pure substrate from that of the total systems [13–15]. Also, the critical macroscopic strain (ε_C, measured in situ using an electrical resistance change method, ERCM [13,14]) characteristic of microcrack formation at the microscopic level, rather than rupture strain or elongation, is used to represent the deformability or ductility for Cu/Cr NMFs. In order to analyze the failure mechanism, the Cu/Cr NMFs tested were cross-sectioned and characterized using an FEI dual-beam focused ion beam/scanning electron microscope (FIB/SEM).

Figure 2(a) shows the dependence of yield strength ($\sigma_{0.2}$) on η for Cu/Cr NMFs with $\lambda = 25$ and 50 nm, respectively. The yield strength is found to be sensitive not only to λ but also to η. $\sigma_{0.2}$ increases remarkably with increasing η up to about 1.0, beyond which it goes up slowly. Within the region of η lower than 1.0, the NMFs with $\lambda = 25$ nm exhibit an $\sigma_{0.2}$ that is obviously larger than those with $\lambda = 50$ nm. This indicates that the strengthening effect is higher at thinner λ because the increased interfaces will suppress or inhibit the movement of dislocations more intensely. When η above 1.0, however, the two kinds of NMFs have almost the same yield strength.

In contrast to the monotonic increase of $\sigma_{0.2}$, the ductility ε_C of the Cu/Cr NMFs reduces monotonically with increasing η (see the experimental results in Fig. 2(b)). The increase in η causes a decrease in the volume fraction of the soft Cu layers, which, in turn, causes the deformation capability of the NMFs to drop. Interestingly, a scaling relationship is revealed for both the two λ when the ductility is depicted with respect to the yield strength, as shown in Figure 2(c). This indicates that, under the constant modulation period or the same number of interfaces, the ductility of NMFs is inversely proportional to the yield strength. The Cu/Cr NMFs with $\lambda = 25$ nm have a scaling slope of -2.8×10^{-3} MPa^{-1}, a factor of 2 higher compared with those with $\lambda = 50$ nm. As mentioned above, the residual stress in the Cu/Cr NMFs is insensitive to both the modulation period and the modulation ratio, and the NMFs with $\lambda = 25$ and 50 nm have similar residual stresses. This indicates that the present experimental results are not predominantly related to the residual stress. Because the NMFs with $\lambda = 25$ nm contain twice as many interfaces as those with $\lambda = 50$ nm, the sharper scaling slope in the former is because the dislocation movement is strongly suppressed by the increased interfaces.

With regard to the metallic multilayers composed of a softer phase and a stiffer phase, flow is controlled by the softer phase and the strengthening is thus closely linked to the characteristic dimension of the softer phase [16,17]. In polycrystalline thin films, the strength of the metallic thin films is determined by the smaller microstructural dimension between the film thickness and the grain size. In the present Cu/Cr NMFs, the Cu layers have a thickness that is much finer than the grain size, so the thickness of the Cu layer is the characteristic dimension controlling the flow behavior of the NMFs. According to the CLS (confined layer slip) model [7,16,17], the applied stress σ_{cls} required to propagate a

glide loop of Burgers vector b confined to one Cu layer is given as

$$\sigma_{cls} = M\frac{\mu^* b}{8\pi h'}\left(\frac{4-\nu}{1-\nu}\right)\ln\frac{\alpha h'}{b} + \frac{f}{h} + \frac{\mu^* b}{L(1-\nu)} = \frac{M\mu^* b}{8\pi h'}\left(\frac{4-\nu}{1-\nu}\right)\ln\frac{\alpha h'}{b} + \frac{f}{h} + \frac{\mu^* V_{Cr}\varepsilon}{m(1-\nu)}, \quad (1)$$

where M is the Taylor factor, h' is the layer thickness parallel to the glide plane, ν is the Poisson ratio for Cu, $\mu^* = \frac{\mu_{Cr}\cdot\mu_{Cu}}{2(V_{Cr}\cdot\mu_{Cu}+V_{Cu}\cdot\mu_{Cr})}$ is the mean shear modulus of Cu/Cr multiplayer, which can be estimated by the shear modulus μ_{Cu} and volume fraction V_{Cu} of the Cu layer and those of the Cr layer, α represents the core cut-off parameter, f is the characteristic interface stress of multilayer, L is the mean spacing of glide loops in a parallel array ($L = b\,m/\varepsilon\,V_{Cr}$ [16]), V_{Cr} is the volume fraction of the Cr layer that is directly related to the modulation ratio (i.e. $V_{Cr} = \eta/(1+\eta)$), ε is the in-plane plastic strain and m is a strain resolution factor of the order of 0.5 for the active slip systems. Tensile data on nanoscale metallic multilayers [8,18] showed a low work hardening rate after the initial 1–2% plastic strain. Misra et al. [7] also found that, using the CLS model, a multilayer flow stress corresponding to a plastic strain of around 1–2% correlated well with the hardness measurement. Following this treatment, an ε of 1% was chosen here to calculate the yield strength of Cu/Cr NMFs by using Eq. (1). With the parameters [7,16,17] of $M = 3$, $\mu_{Cu} =$ 48.3 GPa, $\mu_{Cr} = 115.4$ GPa, $\nu = 0.343$, $b = 0.2556$ nm, $\alpha = 0.2$, f = 3 J m^{-2} and $h' = h_{Cu} = \lambda/(1+\eta)$, the dependence of $\sigma_{0.2}$ on λ as a function of η is quantitatively calculated and is shown in Figure 2(a) as the solid curves. The calculations fit well with the tensile yield strength data in the quickly increasing region (i.e. η below 0.5 for $\lambda = 25$ nm and below 1.0 for $\lambda = 50$ nm). Further increasing η or reducing h_{Cu}, the CLS model is no longer applicable as it overestimates the yield strength too much. In these cases, the dislocations in the very thin Cu layers (thinner than about 20 nm) are deeply pinned by the interfaces. This makes the Cu layers as brittle as the Cr layers, and the NMFs can be seen simply as composites consisting of two hard phases. The yield strength of the NMFs is thus expressed as

$$\sigma_{0.2} = V_{Cu}\,\sigma^*_{Cu} + V_{Cr}\,\sigma^*_{Cr} = \sigma^*_{Cr} - \frac{(\sigma^*_{Cr} - \sigma^*_{Cu})}{(1+\eta)} \quad (2)$$

where σ^*_{Cu} and σ^*_{Cr} are the yield strength of the strongly constrained Cu layers and Cr layers, respectively. Using $\sigma^*_{Cu} = 900$ MPa and $\sigma^*_{Cr} = 1900$ MPa, Eq. (2) gives a good fit to the second stage of the $\sigma_{0.2}$ vs. η curves where the CLS model is no longer applicable (see the dashed curve in Fig. 2(a)). One can see that calculations from the simple mixing law (Eq. (2)) are only related to the volume fraction (or η) of the constituent phases and not to λ, which is also in agreement with the experimental results. The above modeling shows that, increasing η beyond about 1.0 or reducing h_{Cu} down to about 20 nm, the strengthening mechanism in the Cu/Cr NMFs changes from the slide of a single dislocation confined to individual Cu layers to the load-bearing effect, which is similar to cases in some composites. The scaling relationship covers the two regions with different strengthening mechanisms (Fig. 2(c)).

Similar scaling relationships between the ductility and yield strength have been observed in some bulk metallic materials that possess low resistance to strain localization, such as in Al alloys [19]. Macroscopic models [20,21] have been proposed to describe these fracture behaviors, where the fracture criterion was based on some quantity achieving a fixed value when fracture occurs. Typically, the critical stress criterion can be expressed in the form of $\int_0^{\varepsilon_C}\sigma\,d\varepsilon = C$ [19], where ε_C is the effective strain at fracture and σ is the stress, which reaches a critical value C at fracture. The ductility ε_C is expected to scale with the yield strength, since increased yield strength would decrease the strain necessary to achieve the critical stress for fracture in terms of the critical stress criterion. As a result, an increase in yield strength would be expected to produce a proportional decrease in ductility, provided that the strength is achieved with the same microstructure. This is the case for the present metallic multilayers that also have low resistance to strain localization. Here, the "constant microstructure" refers to those microstructural features that would have the same interfaces or the same modulation period, because the number of interfaces is the predominant factor controlling the deformation and fracture in multilayer films. Once the modulation period or the microstructural feature is changed, different scaling lines will be observed. In the current work, the NMFs with $\lambda = 25$ and 50 nm have their own scaling relationships (see Fig. 2(c)). In particular, the NMFs with $\lambda = 25$ nm exhibit a scaling slope that is much sharper than those with $\lambda = 50$ nm. In other words, increasing the yield strength by the same level will cause a greater reduction in the ductility for NMFs with a thinner modulation period. This indicates that the strengthening via interface constraint will sacrifice deformability remarkably, because the movement of dislocations will be strongly suppressed by the increased interfaces.

At a given strength, however, the Cu/Cr NMFs with $\lambda = 25$ nm have a ductility that is higher (not lower) than those with $\lambda = 50$ nm in the CLS-applicable region (left side of Fig. 2(c)). This can be reasonably explained by considering the fracture mechanism in the NMFs composed of alternating soft/hard layers. As illustrated in our previous paper [13], the fracture process of the Cu/Cr NMFs can be described simply as follows: the microcrack first nucleates in the brittle Cr layer and further propagation of the microcracks will be suppressed by the surrounding ductile Cu layers, resulting in microcrack arrest. Whether the microcracks can be suppressed is dependent on two opposite effects: one is the intensity of the stress/strain fields (ISF) ahead of the microcrack tip and the other is the shielding on microcrack propagation by plastic deformation of the Cu layers. The microcracks formed in the Cr layers are the size of the layer thickness, and the ISF ahead of the microcrack tip scales with $\sqrt{h_{Cr}}$ [22] and thus decreases with reducing h_{Cr}. On the other hand, the plastic deformation capability of the Cu layers is heavily dependent on the dislocation movement. In the CLS-applicable region, some dislocations in the Cu layers are movable and the Cu layers have some deformation capability to

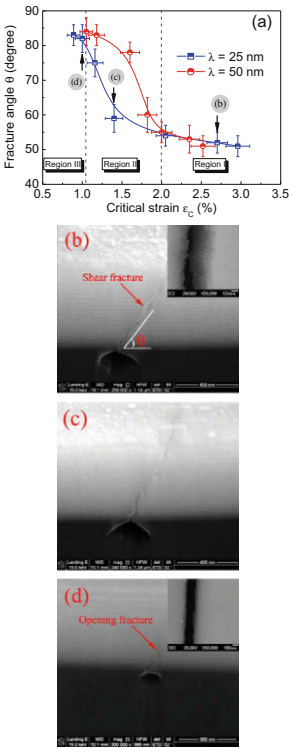

Figure 3. (a) Dependence of θ on ε_C for the Cu/Cr NMFs with $\lambda = 25$ and 50 nm. The curves are visual guides. The SEM cross-sectional images in (b), (c) and (d) typically showing shear mode, shear + opening mixing mode and opening mode in $\lambda = 25$ nm Cu/Cr NMFs with $\eta = 0.2$, $\eta = 0.5$ and $\eta = 2$, respectively. The insets show the corresponding SEM plan view images of the NMFs, which can be used to further demonstrate the shear and opening fracture mode.

shield the propagation of tiny microcracks. The thinner the microcrack size or h_{Cr}, the more possible it is for the Cu layers to arrest the microcracks. The Cu/Cr NMFs with $\lambda = 25$ nm have an h_{Cr} that is only half that for $\lambda = 50$ nm and therefore show greater ductility. Beyond the CLS-applicable region, the NMFs can be equivalent to composites consisting of alternate brittle Cu layers and brittle Cr layers. Here, the larger number of weak interfaces will remarkably degrade the deformability for $\lambda = 25$ nm, causing its ductility to be lower than that for $\lambda = 50$ nm.

Further microstructural observations were carried out to relate the ductility to the fracture behaviors. Figure 3(a) shows the experimentally determined fracture angle θ (θ is defined as the angle between the macrocracking direction and the horizontal direction; see Fig. 3(b)) as a function of the ductility ε_C. A higher ε_C corresponds to a smaller θ, and the $\theta - \varepsilon_C$ curves can be divided into three regions. In region I, where ε_C is above ~2.0, θ changes slowly with ε_C and the curves of the two NMFs with $\lambda = 25$ and 50 nm are almost equal. The microcracks initiated in the Cr layers can be easily arrested by the surrounding deformable Cu layers, causing the NMFs fracture in a shear mode (Fig. 3(b)) with $\theta \sim 52 \pm 3°$. In region III, where ε_C is below ~1.0, θ again changes slowly with ε_C, and the curves of the two NMFs with $\lambda = 25$ and 50 nm are close. In this region, the Cu layers are strongly constrained and have almost no deformation capability to resist the microcrack propagation. Fracture in the two NMFs is the same opening mode (Fig. 3(d)), where θ is $\sim 83 \pm 3°$. In the intermediate region II, however, the NMFs fracture in a shear + opening mixing mode (Fig. 3(c)), which makes θ varies significantly with ε_C. In particular, the θ of the NMFs with $\lambda = 50$ nm is obviously higher than that of NMFs with $\lambda = 25$ nm in this region. This further indicates that the larger microcracks (larger h_{Cr}) in the $\lambda = 50$ nm Cu/Cr NMFs are more difficult to arrest by the surrounding Cu layers, in broad agreement with the discussions on Figure 2(c).

Finally, it should be noted that the scaling relationship between ductility and yield strength revealed here could be useful when considering the optimization of a multilayer microstructure for the best combination of strength and fracture resistance, especially in connection with the prediction of strength by using dislocation models.

The authors thank S.W. Guo for her help with the TEM operation. This work was supported by grants from NSFC (50971097), 973 Program of China (2010CB631003) and 111 Project of China (B06025).

[1] A. Misra, H. Kung, Adv Eng Mater 3 (2001) 217.
[2] Y.F. Chen, Y.F. Mei, R. Kaltofen, J.I. Mönch, J. Schumann, J. Freudenberger, H.-J. Klauß, O.G. Schmidt, Adv Mater 20 (2008) 3224.
[3] M.J. Demkowicz, R.G. Hoagland, J.P. Hirth, Phys Rev Lett 100 (2008) 136102.
[4] I. Bakonyi, L. Péter, Prog Mater Sci (2009), doi:10.1016/j.pmatsci.2009.07.001.
[5] G.S. Was, T. Foecke, Thin Solid Films 286 (1996) 1.
[6] A. Misra, M. Verdie, Y.C. Lu, H. Kung, T.E. Mitchell, M. Nastasi, J.D. Embury, Scripta Mater 39 (1998) 555.
[7] A. Misra, J.P. Hirth, R.G. Hoagland, Acta Mater 53 (2005) 4817.
[8] H. Huang, F. Spaepen, Acta Mater 48 (2000) 3261.
[9] A. Misra, R.G. Hoagland, J Mater Res 20 (2005) 2046.
[10] E. Arzt, Acta Mater 46 (1998) 5611.
[11] B.M. Clemens, W.D. Nix, V. Ramaswamy, J Appl Phys 87 (2000) 2816.
[12] Th. Detzel, N. Memmel, Phys Rev B 49 (1994) 5599.
[13] J.Y. Zhang, G. Liu, X. Zhang, G.J. Zhang, J. Sun, E. Ma, Scripta Mater 62 (2010) 333.
[14] R.M. Niu, G. Liu, C. Wang, G. Zhang, X.D. Ding, J. Sun, Appl Phys Lett 90 (2007) 161907.
[15] D.Y.W. Yu, F. Spaepen, J Appl Phys 95 (2004) 2991.
[16] J.D. Embury, J.P. Hirth, Acta Metall Mater 42 (1994) 2051.
[17] M.A. Phillips, B.M. Clemens, W.D. Nix, Acta Mater 51 (2003) 3157.
[18] N. Mara, A. Sergueeva, A. Misra, A.K. Mukherjee, Scripta Mater 50 (2004) 803.
[19] D.J. Lloyd, Scripta Mater 48 (2003) 341.
[20] M.G. Cockcrof, D.J. Latham, JIM 96 (1968) 33.
[21] M. Jain, J. Allin, D.J. Lloyd, J Int Mech Sci 41 (1999) 1273.
[22] R.W. Hertzberg, Deformation and fracture mechanics of engineering materials, John Wiley & Sons, New York, 1989.